

## The influence of Cu content on high temperature corrosion behavior of heat - resistant molten salt steel

Hong Li<sup>1</sup>, Hui Zhang<sup>1</sup>,  
Chengzhi Zhao<sup>1,2</sup>, Hexin Zhang<sup>1,2</sup>,  
Qiang Wang<sup>1</sup>

<sup>1</sup> College of Materials Science and Chemical Engineering, Harbin Engineering University, No. 145 Nantong Avenue, 150001, Harbin, Heilongjiang, China.

<sup>2</sup> Key Laboratory of Superlight Materials and Surface Technology of Ministry of Education, Harbin Engineering University, No. 145 Nantong Avenue, 150001, Harbin, Heilongjiang, China.

e-mail: Liandting@yeah.net, july0828@hrbeu.edu.cn, zhaochengzhi@hrbeu.edu.cn, zhanghx@hrbeu.edu.cn, 18845631880@163.com

---

### ABSTRACT

This work studies the high temperature corrosion behavior of new heat-resistant steel with salt coating method of 75%Na<sub>2</sub>SO<sub>4</sub>+25%NaCl coating on the steel surface at 700°C. The chemical composition of corrosion products and surface morphology of the corrosion layer were analyzed using X-ray diffractometer (XRD), scanning electron microscopy (SEM), energy dispersive spectroscopy (EDS) and investigate the effect of Cu content on high temperature corrosion behavior of heat resistant steel. The results show that the thermal corrosion kinetics curve of tested steel follows the parabolic law and the surface is composed of Fe<sub>2</sub>O<sub>3</sub> and FeCr<sub>2</sub>O<sub>4</sub>. The corrosion layer were divided into two layers, the outer layer was loose and porous while the inner layer was dense and continuous. The structure of the oxide film consists of various protective oxide films; with increasing of Cu content, the high-temperature corrosion resistance of heat-resistant steel was improved and the thickness of the corrosion layer was decreased which led to improving the bonding strength between the inner layer and the matrix. The results of EDS analysis shows that Cu elements can promote the outward diffusion of Cr elements to oxidation of the steel to form a Cr<sub>2</sub>O<sub>3</sub> protective oxide film for preventing the diffusion of chlorine elements, oxygen elements into the interior toward the steel with slow down the process of "activation oxidation", reduce the sensitivity of intergranular corrosion and achieve the function of protecting materials.

**Keywords:** Heat-resistant steel. Thermal corrosion. Molten salt. Corrosion layer.

---

### 1. INTRODUCTION

The super supercritical unit with high steam parameters has the advantages of high efficiency, cleanliness, economy, safety and so on. It has become the main development direction of the thermal power unit in the world [1]. In the future unit parameters will reach temperature of 700°C and 30 MPa, or even more aggressive parameters [2]. Obviously, the existing boiler steel can no longer meet its service requirements, so we must develop heat-resistant materials that are suitable for aggressive parameters, and ensure the reliable operation of the unit. Ferritic heat-resistant steel for boiler is widely used in supercritical generating units with high steam parameters because of its excellent comprehensive performance [3-6] and T91 as the representative of this steel, it has been become the most extensive steel grade in the world supercritical power plant at the same time, it is also used as a benchmark for developing high steam parameter steel [7, 8].

At present, there is still a gap between the ferritic heat-resistant steel and the advanced austenitic heat-resistant steel in the heat-resistance temperature [9]. At the same time, the fuel of the thermal power unit contains sulfur, chlorine and other harmful substances, it forms sulfides, sulfates, chlorides and the like after burning, which causes high temperature corrosion on the materials [10], resulting in the frequent occurrence of boiler "four tubes" explosion accidents. Relevant studies have shown that [11-16]: corrosion is significantly accelerated above the melting point of the molten salt, and below the melting point, oxidation is accelerated; under the melting condition, NaCl will destroy the protective oxide film, which is the main reason for accelerating the alloy corrosion, especially under the effect of chlorine salt and sulphate, the protective oxide

film is more likely to be destroyed, corrosion is more serious. At present, there are a lot of studies on thermal corrosion at home and abroad after high temperature water vapor and coating [17-20], and many mechanisms are proposed. However, none of them can fully explain the corrosion model of high temperature chlorination corrosion, and this high temperature chlorination corrosion experiment lack of experimental data, restricting the development of high temperature corrosion mechanism.

In this paper, T91 steel is taken as the benchmark, and its chemical composition is optimized by JMatPro thermodynamic simulation, and developed a new type of ferritic heat-resistant steel, improving high-temperature oxidation resistance of heat-resistant steel and the hot corrosion behavior of steel in molten salt. Coated salt corrosion method [21,22] was used to study the corrosion behavior of a new type of heat-resistant steel in a molten salt environment with mass fraction of 75% Na<sub>2</sub>SO<sub>4</sub> + 25% NaCl under temperature of 700°C in the atmosphere. Analysis of the corrosion products phase composition, sectional features, and elements distribution, the influence of Cu content on the thermal corrosion behavior of heat-resistant steel was performed. The hot corrosion mechanism of molten salt of new heat-resistant steel were analyzed and discussed, which provides theoretical basis and experimental basis for the development of new boiler steel to promote the development of ultra-supercritical power generation technology.

## 2. MATERIALS AND METHODS

### 2.1 Experimental materials

The samples were obtained using high vacuum arc melting furnace and smelting with different Cu content. After the smelting completed, the sample was prepared to the small pieces with the size of  $R \geq 15$ mm. The chemical composition of the as-cast steels were carried out using the German Spike direct reading spectrometer as shown in Table 1. The heat treatment was conducted on a high-temperature box type resistance RJX-18-13 resistance furnace. The samples were heat-treated at 1050°C for 45 minutes, and removed sample from furnace for air cooling and then placed in a furnace at 770°C for 2 hours with 80°C/h speed furnace cooling to 300°C and then cooled down to room temperature. The test steel was processed into a small size of 20mm×10mm×2mm by wire cutting, after grinding, fine grinding, polishing, and then cleaned twice with ethanol and acetone, and dried for use.

**Table 1:** Chemical compositions of heat-resistant steels (mass fraction %)

STEEL NUMBER	C	Si	Mn	Cr	Ni	Mo	Cu	Al	V	Nb
#1	0.09	0.24	1.15	9.65	1.43	0.84	0.86	1.01	0.29	0.09
#2	0.10	0.25	1.17	9.61	1.47	0.85	1.72	1.07	0.28	0.08
#3	0.11	0.24	1.19	9.64	1.42	0.82	2.54	1.05	0.28	0.09

### 2.2 Experiment method

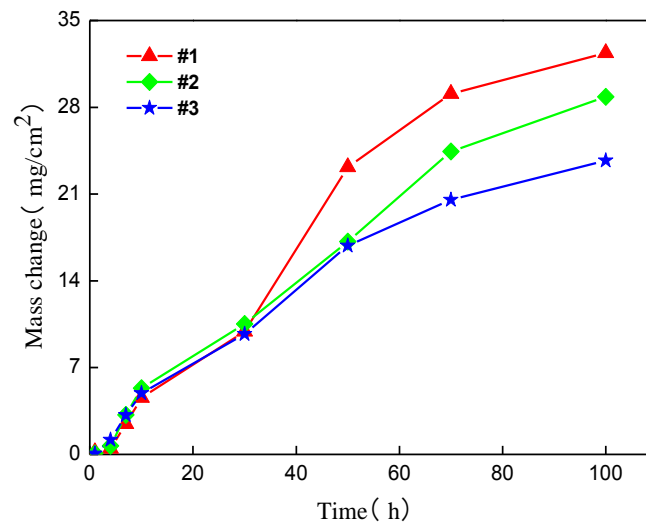
Measuring the size and weighing of the samples and put the samples on a clean plate and heat preservation under 200°C for 5 min, and then evenly coated with a saturated salt solution of 75% Na<sub>2</sub>SO<sub>4</sub>+25% NaCl on the samples surface, drying and then make its surface deposition 10 mg/cm<sup>2</sup> salt membrane. Put sample into the alumina crucible which is burned till constant weight and put them into the muffle heating resistance furnace SM-28-10 for high temperature corrosion test, the furnace door has 10 mm small holes to ensure that the furnace has enough oxygen.

The test temperature selected for corrosion experiment was 700°C and the time is 100h. One sample was taken at the time points of 1, 4, 7, 10, 30, 50, 70 and 100h respectively. The remaining sample is continued to be etched at high temperature, after cooling to room temperature for 25min, the weight gain is weighed by the electronic analytical balance with the accuracy of  $1 \times 10^{-4}$ g, select three samples for parallel experiments, the results averaged. The discontinuous weight gain method was used to draw the corrosion kinetic curve according to the corrosion weight gain per unit area and corrosion time, X-ray diffractometer (XRD) were analyzed the qualitative of samples after corrosion with Cu K $\alpha$  radiation ( $\lambda=1.5406\text{\AA}$ ) and 2 $\theta$  scan between 20° to 90°. The surface morphology of the samples for corrosion section were observed using FEI Quanta F-type field emission scanning electron microscope (SEM), energy dispersive spectroscopy (EDS) analysis was also combined with high temperature molten salt corrosion mechanism.

### 3. RESULTS

#### 3.1 Corrosion kinetics curve

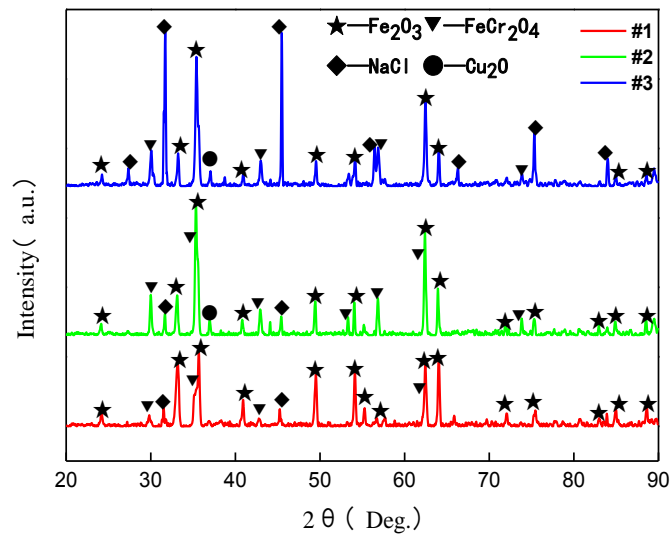
The corrosion kinetics of the samples after being eroded for 100h in the deposited salt film of 75%  $\text{Na}_2\text{SO}_4$ +25% $\text{NaCl}$  (mass fraction) under the temperature of 700°C is shown in Fig.1. The composite deposit was used in the experiment had a melting point of about 675°C and the eutectic melting point at 630°C [23] while the deposition salt was liquid at 700 °C. Fig.1 shows the trend of corrosion weight gain of the three types of samples were similar as follows in the parabolic rule. It is shown that the heat-resistant steel had certain high temperature corrosion resistance. Meanwhile, the increase of Cu content in the steel is beneficial to improve the hot corrosion resistance of molten steel. The corrosion kinetics curve were divided into two phases, the first phase was increased rapidly and the second phase was increased slowly. The reasons for this are as follows: in the early stage of corrosion, high temperature oxidation plays a leading role, and a dense and continuous protective oxide film was rapidly formed on the surface. After the oxide film completely covers on the substrate, the high temperature corrosion transition takes a leading role, with the destruction of the oxide film by the deposited salt, the samples show a gradual weight gain under the dual action of oxidation and corrosion due to the presence of protective oxide film in the early stage, the weight gain trend was slowed down.



**Figure 1:** High temperature corrosion kinetics curve of test steel

#### 3.2 XRD analysis of corrosion products

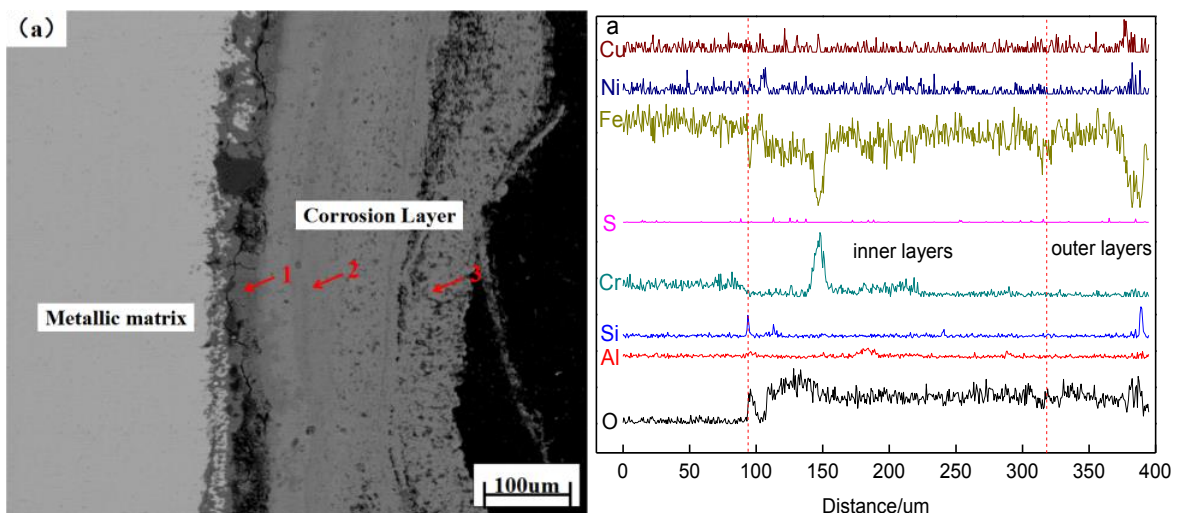
The XRD patterns of the surface corrosion products of the test steel after 100 h corrosion in molten salt are shown in Fig.2. It can be seen that the corrosion products of the surface after corrosion are mainly composed of  $\text{Fe}_2\text{O}_3$  and  $\text{FeCr}_2\text{O}_4$ , in the process of corrosion, the deposited salt will pass through the oxide film, which reacts with the oxide film and the matrix, resulting chloride will be oxidized to the stable phase of the metal oxide [24]. The Gibbs free energy of reaction of iron chloride with oxygen was large. Therefore, the iron oxide is eventually formed and covered on the surface of other metal oxides and the surface of the sample contains some residual deposited salt according to the diffraction peak strength of the deposited salt. It can be concluded that there is less deposited salt on the surface of #1 sample, but there is a lot of sedimentary salt on the surface of #3 sample, this indicates that the corrosion effect of sedimentary salt on #3 sample was weaker than #1 and #2 sample.



**Figure 2:** XRD map of surface products after 100h corrosion in test steel

### 3.3 Characteristics of corrosion section morphology

The corrosion morphology on the surface and elements distribution of the three sample test after 100h and corrosion temperature at 700°C are shown in Fig.3. According to the thickness of the corrosion layer, it is found that the #3 test steel had the best condition of high temperature corrosion resistance to molten salt, with the increases of Cu content is beneficial to the improvement of the high temperature corrosion resistance of the heat-resistant steel. After high temperature corrosion of molten salt, the corrosion layer was divided into two layers, the outer layer was porous and the inner layer was dense. The bond between the inner layer and the matrix was weak, there are micro cracks, holes, and the bond with the matrix was effectively improved with increased of Cu content are shown in Fig.3 (c). It can be seen from the figure that there are intergranular corrosion in all three kinds of test steels. With the increase of Cu content, the sensitivity of intergranular corrosion was reduced, and the degree of intergranular corrosion is weakened. According to the corrosion layer can be seen that the outer layer is mainly iron-rich oxide ( $\text{Fe}_2\text{O}_3$ ), while the inner layer of iron ions are largely absent, mainly composed of chromium-rich oxide ( $\text{Cr}_2\text{O}_3$ ) and a small amount of  $\text{Al}_2\text{O}_3$  oxide, with increase of Cu element promotes the outward diffusion of chromium, a thicker  $\text{Cr}_2\text{O}_3$  oxide film was formed.  $\text{FeCl}_3$  was formed during the corrosion of iron, the boiling point is only at 316°C, it volatilizes to the outer layer and is oxidized to unprotected  $\text{Fe}_2\text{O}_3$ , chloride ions will be released again to react with the metal elements in the alloy.



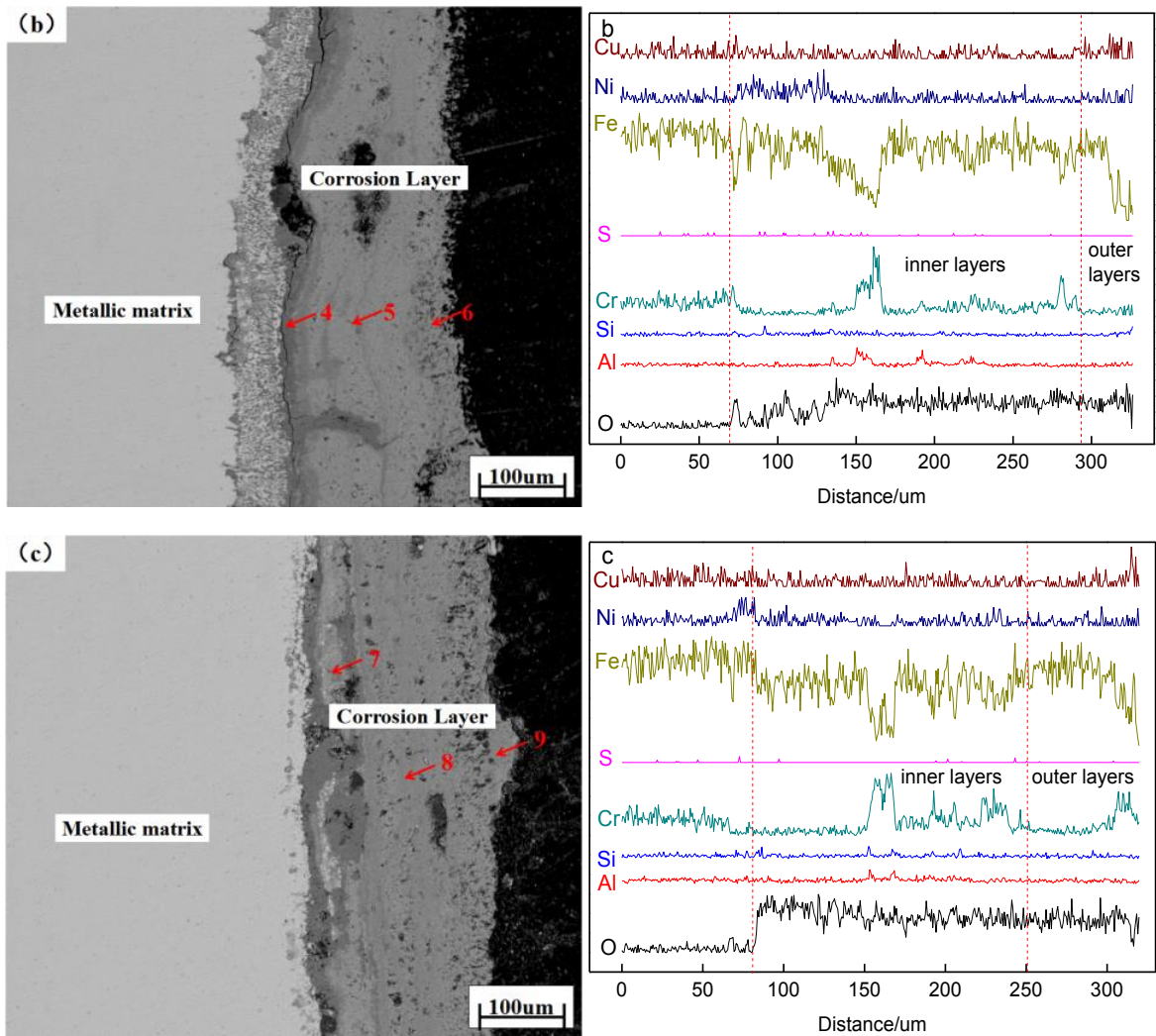


**Figure 3:** Features of section morphology and distribution of elements after 100h corrosion of test steel (a #1;b #2;c #3)

Table 2 shows the results of EDS analysis of different regions in the three samples of corrosion layers. Combined with the element distribution in Fig.3 of corrosion layer, it can be seen that the main change elements in the corrosion layer are Al, Si, Cr, Fe and O. The oxides formed by aluminum, silicon and chromium are usually dense, which protect the material. According to the results in Fig.3 and Table 2, it can be concluded that the protective oxide film formed by three elements (Al, Si, Cr) is mainly concentrated on the inner layer of corrosion layer for protecting the matrix. With the mass fraction of Fe element in different areas of corrosion layer, the degree of chlorination reaction of #1 sample was the largest and, showing an increasing trend from the inner layer to outer layer. The performance of #2 sample was not obvious, which indicates that the increase of Cu content can inhibit the reaction of chlorination to a certain extent. However, the #3 sample shows a decreasing trend while the outer layer was found to be rich in chromium (15.86%), this is because of the protective oxide film formed by the dominant role of high temperature oxidation in the early stage of corrosion has not been completely destroyed, still protect the materials, the progress of the chlorination reaction is suppressed or delayed.

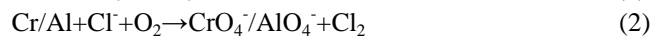
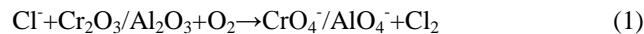
**Table 2:** EDS analysis of different regions of high temperature corrosion section (mass fraction %)

FIGURE3	LOCATION	O	Al	Si	Cr	Fe	Ni	Cu
(a)	1	8.79	2.01	1.31	8.91	53.51	2.23	1.55
	2	18.57	1.11	0.25	5.84	58.16	2.99	1.07
	3	18.14	0	0.29	0.73	68.11	1.17	1.55
(b)	4	18.28	0.91	1.00	0.68	61.85	1.05	1.40
	5	17.36	4.21	0.28	5.62	54.58	1.08	0.69
	6	17.76	0.09	0.29	0.67	62.45	1.09	1.08
(c)	7	18.81	0.16	2.84	3.20	54.91	0.95	0.98
	8	20.85	0.64	0.27	9.45	50.99	0.90	1.13
	9	20.06	0.23	0.34	15.86	44.10	1.98	0.78

#### 4. DISCUSSION

The explanation of the mechanism of high temperature chloride corrosion, we more agree with the mechanism of "activated oxidation" [25], which includes complex processes such as chemical reaction, interface reaction and dissolution of oxides [26]. Because of the high activity of chlorine, it can be reacted with all the sample at high temperatures, chlorides produced after chlorination had a lower melting point and higher vapor pressure than metal oxides [27] and lead to a rapid consumption of Al and Cr in the alloy. In addition, it will increase the protective oxide film ( $\text{Al}_2\text{O}_3$ ,  $\text{Cr}_2\text{O}_3$ ) cracking and peeling tendency.

In this experiment, at the high temperature oxidation plays a leading role in the initial stage of corrosion, oxygen selectively oxidize with test steel by depositing salt film [28] which results in dense of  $\text{Cr}_2\text{O}_3$ ,  $\text{Al}_2\text{O}_3$  and  $\text{SiO}_2$  protective oxide films. At the same time,  $\text{MoO}_3$ ,  $\text{V}_2\text{O}_5$  and other refractory metal oxide are also generated [29]. Subsequently, the NaCl in the molten state will pass through the oxide film and react with the initial  $\text{Cr}_2\text{O}_3$  and  $\text{Al}_2\text{O}_3$ , as well as the Cr and Al in the alloy as follows [30]:



And the reaction ability of the refractory metal oxide to the oxygen ion in the molten  $\text{Na}_2\text{SO}_4$  is stronger, and the following reaction will take place [31]:



The form metal chlorine produced by reactions on Eqs. (1) and (2) diffuses inwardly through the oxide film gaps and holes and forms chlorides with iron and chromium in the alloy, while  $\text{FeCl}_3$  is volatile and oxidized to non-protective oxide in the outward diffusion, chlorine ions are released again, and they continue to react with metal elements in the alloy. As shown in reactions Eqs. (5) and (6):



During this process of corrosion, the elemental chlorine in the deposited salt plays an autocatalytic role [32, 33]. This catalytic action can be maintained with very little chlorine content, and the outward transport of metal chlorides because of many defects and voids in the protective film, providing many channels for the inward transport of chlorine and the outward diffusion of chloride, accelerating the movement of gaseous species, making the oxide film becomes a very loose oxide film, thus losing the original protective effect.

Since reactions Eqs. (3) and (4) consume oxygen ions at the molten salt and the alloy interface, the molten  $\text{Na}_2\text{SO}_4$  is acidic near the interface, and the oxide film decomposes in an acidic mode and loses its protective property [31]. Sulfate ions in molten  $\text{Na}_2\text{SO}_4$  decompose at high temperature and react with the alloy to form sulfides [34,35], As shown in the results of the elemental analysis in Fig.3, there is a certain amount of



S element in the oxide film and the surface has undergone a sulfurization reaction while sulfides have higher defects, larger volumetric ratios (PBR), and are prone to cracking and spalling, accelerating the failure of materials.

With the increasing of Cu content in the steel, the high temperature corrosion resistance of the molten salt was improved and the bond between the inner layer and the matrix is also effectively improved. The reason for this is that the Cu element promotes the outward diffusion of the Cr element to form  $\text{Cr}_2\text{O}_3$  protective oxide film, hinders the inward diffusion of chloride ions, slowing the process of "activated oxidation". At the same time, the increase of Cu element reduces the intergranular corrosion sensitivity of the test steel, improves the bond between the oxide film and the matrix, and improves the bonding strength of them.

## 5. CONCLUSIONS

The hot corrosion kinetics curves of the new heat-resistant steel at temperature of 700 °C with 75%  $\text{Na}_2\text{SO}_4$  + 25%NaCl deposition salt environment follows the parabolic law and show certain high temperature corrosion resistance. After corrosion, the surface of the samples are mainly composed of  $\text{Fe}_2\text{O}_3$  phase, the corrosion layer were divided into two layers, the outer layer is loose and porous which mainly composed of  $\text{Fe}_2\text{O}_3$  "non-protective" oxide film while the inner layer is more dense and continuous, mostly  $\text{Al}_2\text{O}_3$ ,  $\text{Cr}_2\text{O}_3$ ,  $\text{SiO}_2$  protective oxide film. With the increase of Cu content in steel, the diffusion of Cr elements was promoted, and  $\text{Cr}_2\text{O}_3$  oxide film with protective effect was formed, the increase of Cu element effectively reduces the intergranular corrosion sensitivity of the test steel, which improves the corrosion resistance of materials and enhances the bonding strength between inner oxide film and matrix.

## 6. ACKNOWLEDGMENTS

This article is Supported by The Fundamental Research Funds for the Central Universities of China (No.HEUCFP201719 and No.HEUCFP201731) and Science and technology plan projects in jiangsu province of China(NO.BE2017105).

## 7. BIBLIOGRAPHY

- [1] HALD, J., VISWANATHAN, V., ABE, F., "Energy drivers for materials research and development", *Energy Materials Materials Science & Engineering for Energy Systems*, v. 1, n. 1, pp. 1-6, Nov. 2006.
- [2] VISWANATHAN, R., HENRY, J.F., TANZOSH, J., *et al.*, "US Program on Materials Technology for Ultrasupercritical Coal-Fired Boilers", In: *Conference on Advances International in Materials Technology*, pp. 1-15, Jan. 2008.
- [3] UWABA, T., UKAI, S., NAKAI, T., *et al.*, "Properties of friction welds between 9Cr-ODS martensitic and ferritic–martensitic steels", *Journal of Nuclear Materials*, v. 367-370, n. s, pp. 1213-1217, Aug. 2007.
- [4] OÑORO, J., "Weld metal microstructure analysis of 9–12% Cr steels", *International Journal of Pressure Vessels & Piping*, v. 83, n. 7, pp. 540-545, Jul. 2006.
- [5] SCHROER, C., KONYS, J., "Quantification of the Long-Term Performance of Steels T91 and 316L in Oxygen-Containing Flowing Lead-Bismuth Eutectic at 550°C", *Journal of Engineering for Gas Turbines & Power*, v. 132, n. 8, pp. 671-679, Jul. 2009.
- [6] MARTINELLI, L., BALBAUD CÉLÉRIER, F., "Modelling of the oxide scale formation on Fe - Cr steel during exposure in liquid lead - bismuth eutectic in the 450–600 °C temperature range", *Materials & Corrosion*, v. 62, n. 6, pp. 531-542, Jun. 2015.
- [7] SAMANTARAY, D., MANDAL, S., BHADURI, A.K. "Characterization of deformation instability in modified 9Cr–1Mo steel during thermo-mechanical processing", *Materials & Design*, v. 32, n. 2, pp. 716-722, Feb. 2011.
- [8] SAMANTARAY, D., MANDAL, S., BHADURI, A.K., "A comparative study on Johnson Cook, modified Zerilli–Armstrong and Arrhenius-type constitutive models to predict elevated temperature flow behaviour in modified 9Cr–1Mo steel", *Computational Materials Science*, v. 47, n. 2, pp. 568-576, Dec. 2009.
- [9] HA, V.T., JUNG, W.S., "Creep behavior and microstructure evolution at 750 °C in a new precipitation-strengthened heat-resistant austenitic stainless steel", *Materials Science & Engineering A*, v. 558, pp. 103-111, Dec. 2012.
- [10] SKRIFVARS, B.J., *et al.*, "Corrosion of superheater steel materials under alkali salt deposits Part 1: The

- effect of salt deposit composition and temperature”, *Corrosion Science*, v. 50, n. 5, pp. 1274-1282, May. 2008.
- [11] HIRAMATSU, N., UEMATSU, Y., TANAKA, T., *et al.*, “Effects of alloying elements on NaCl-induced hot corrosion of stainless steels”, *Materials Science & Engineering A*, v. 120, n. 1, pp. 319-328, Nov. 1989.
- [12] WANG, C.J., CHANG, Y.C. “TEM Study of the Internal Oxidation of an Fe–Mn–Al–C Alloy After Hot Corrosion”, *Oxidation of Metals*, v. 57, n. 3, pp. 363-378, Apr. 2002.
- [13] WANG, C.J., HE, T.T., “Morphological Development of Subscale Formation in Fe–Cr–(Ni) Alloys with Chloride and Sulfates Coating”, *Oxidation of Metals*, v. 58, n. 3, pp. 415-437, Oct. 2002.
- [14] WANG, F., SHU, Y., “Influence of Cr Content on the Corrosion of Fe–Cr Alloys: The Synergistic Effect of NaCl and Water Vapor”, *Oxidation of Metals*, v. 59, n. 3, pp. 201-214, Apr. 2003.
- [15] SHU, Y., WANG, F., WU, W., “Corrosion Behavior of Pure Cr with a Solid NaCl Deposit in O<sub>2</sub> Plus Water Vapor”, *Oxidation of Metals*, v. 54, n. 5, pp. 457-471, Dec. 2000.
- [16] WANG, C.J., CHANG, Y.C., “NaCl-induced hot corrosion of Fe–Mn–Al–C alloys”, *Materials Chemistry & Physics*, v. 76, n. 2, pp. 151-161, Aug. 2002.
- [17] LIU, G., WANG, C., YU, F., *et al.*, “Evolution of Oxide Film of T91 Steel in Water Vapor Atmosphere at 750 °C”, *Oxidation of Metals*, v. 81, n. 3, pp. Apr, Feb. 2014.
- [18] GURR, M., BAU, S., BURMEISTER, F., *et al.*, “Investigation of the corrosion behavior of Ni/Al multilayer coatings in hot salt melts”, *Surface & Coatings Technology*, v. 279, pp. 101-111, Aug. 2015.
- [19] KALVALA, P.R., AKRAM, J., MISRA, M., *et al.*, “Low temperature frictions stir welding of P91 steel”, *Defence Technology*, v. 12, n. 4, pp. 285-289, Dec. 2016.
- [20] SHIBLI, A., F. STARR., “Some aspects of plant and research experience in the use of new high strength martensitic steel P91”, *International Journal of Pressure Vessels & Piping*, v. 84, n. 1, pp. 114-122, Jan. 2007.
- [21] MAHOBIA, G.S., PAULOSE, N., MANNAN, S.L., *et al.*, “Effect of hot corrosion on low cycle fatigue behavior of superalloy IN718”, *International Journal of Fatigue*, v. 59, n. 59, pp. 272-281, Feb. 2014.
- [22] MAHOBIA, G.S., PAULOSE, N., SINGH, V., “Hot Corrosion Behavior of Superalloy IN718 at 550 and 650 °C”, *Journal of Materials Engineering & Performance*, v. 22, n. 8, pp. 2418-2435, Aug. 2013.
- [23] DEB, D., IYER, S.R., RADHAKRISHNAN, V.M. “A comparative study of oxidation and hot corrosion of a cast nickel base superalloy in different corrosive environments”, *Materials Letters*, v. 29, n. 1, pp. 19-23, Nov. 1996.
- [24] SHINATA, Y., “Accelerated oxidation rate of chromium induced by sodium chloride”, *Oxidation of Metals*, v. 27, n. 5, pp. 315-332, Jun. 1987.
- [25] HOFMEISTER, M., KLEIN, L., MIRAN, H., *et al.*, “Corrosion behaviour of stainless steels and a single crystal superalloy in a ternary LiCl–KCl–CsCl molten salt”, *Corrosion Science*, v. 90, pp. 46-53, Jan. 2015.
- [26] LIU, S., LIU, Z., WANG, Y., *et al.*, “A comparative study on the high temperature corrosion of TP347H stainless steel, C22 alloy and laser-cladding C22 coating in molten chloride salts”, *Corrosion Science*, v. 83, n. 6, pp. 396-408, Jun. 2014.
- [27] LI, Y., AL-OLMARY, M., *et al.*, “The Corrosion of Various Materials under Chloride Deposits at 623-723K in Pure Oxygen”, *High Temperature Materials & Processes*, v. 21, n. 1, pp. 11-24, Jun. 2002.
- [28] LIU, G., WANG, C., YU, F., *et al.*, “Evolution of Oxide Film of T91 Steel in Water Vapor Atmosphere at 750 °C”, *Oxidation of Metals*, v. 81, n. 3, pp. 383-392, Apr. 2014.
- [29] TANG, Z., HU, R., LI, J., “Isothermal Oxidation Behavior of Ni-20Cr-18W Superalloy at 1100 °C”, *Rare Metal Materials & Engineering*, v. 41, n. 12, pp. 2081-2085, Dec. 2012.
- [30] LI, P., QIN, P., ZHAO, J., *et al.*, “Hot Corrosion Behavior of Super304H Coated Na<sub>2</sub>SO<sub>4</sub>-25%NaCl Film”, *Journal of Materials Engineering*, v. 44, n. 2, pp. 69-74, May. 2016.
- [31] LI, M. “Hot corrosion”, In: *Hot corrosion mechanism, High temperature corrosion of metals*, 1 ed., chapter 10, Bei Jing, CHINA, Metallurgical Industry Press, 2001.
- [32] OTSUKA, N., “Effects of fuel impurities on the fireside corrosion of boiler tubes in advanced power generating systems—a thermodynamic calculation of deposit chemistry”, *Corrosion Science*, v. 44, n. 2, pp. 265-283, Feb. 2002.



[33] BENDER, R., SCHÜTZE, M., “The role of alloying elements in commercial alloys for corrosion resistance in oxidizing - chloridizing atmospheres. Part I: Literature evaluation and thermodynamic calculations on phase stabilities”, *Materials & Corrosion*, v. 54, n. 8, pp. 567-586, Aug. 2003.

[34] ZHAO, S., XIE, X., SMITH, G.D., *et al.*, “The corrosion of INCONEL alloy 740 in simulated environments for pulverized coal-fired boiler”, *Materials Chemistry & Physics*, v. 90, n. 2, pp. 275-281, Apr. 2005.

[35] TSAUR, C.C., ROCK, J.C., WANG, C-J., *et al.*, “The hot corrosion of 310 stainless steel with pre-coated NaCl/Na<sub>2</sub>SO<sub>4</sub> mixtures at 750 °C”, *Materials Chemistry & Physics*, v. 89, n. 2, pp. 445-453, Feb. 2005.

#### ORCID

Hong Li <https://orcid.org/0000-0002-2522-7098>

Hui Zhang <https://orcid.org/0000-0003-1720-490X>

Chengzhi Zhao <https://orcid.org/0000-0002-4323-0098>

Hexin Zhang <https://orcid.org/0000-0002-5793-5013>

Qiang Wang <https://orcid.org/0000-0002-7429-1678>